

# Dynamical Janssen effect on granular packings with moving walls

Yann Bertho, Frédérique Giorgiutti-Dauphiné and Jean-Pierre Hulin

Laboratoire FAST, UMR 7608, Bât. 502, Université Paris-Sud, 91405 Orsay Cedex (France)

Apparent mass ( $M_{\text{app}}$ ) measurements at the bottom of granular packings inside a vertical tube in relative motion are reported. They demonstrate that Janssen's model is valid over a broad range of velocities  $v$ . The variability of the measurements is lower than for static packings and the theoretical exponential increase of  $M_{\text{app}}$  with the height of the packing is precisely followed (the corresponding characteristic screening length is of the order of the tube diameter). The limiting apparent mass at large heights is independent of  $v$  and significantly lower than the static value.

PACS numbers: 45.70.-n, 81.05.Rm, 83.80.Fg

Dense, dry vertical particle flows in channels are frequently encountered in industrial processes such as the emptying of silos or pneumatic transport [1]. Particle fraction and velocity variations in these flows depend largely on interaction forces either between the particles or between the particles and the channel walls [2, 3]. The present work studies experimentally such forces in the case of a granular packing globally at rest but in relative motion with respect to an upwards moving tube. These force distributions have been extensively studied by many authors for static or quasi-static packing in tubes [4, 5, 6, 7, 8, 9, 10] or other configurations [11, 12, 13, 14]. The pioneering work of Janssen demonstrated in particular that the effective weight at the bottom end of a container reaches exponentially a limit when the height of a static packing increases: this is due to the shielding effect of contact forces between grains redirecting the weight towards the side walls. Vanel *et al.* [15] measured the apparent weight of packed beads moving very slowly down a vertical tube ( $v = 20 \mu\text{m s}^{-1}$ ): these experiments indicate that the weight increases during the displacement before reaching a constant value but the influence of the height of the packing was not investigated. In this work we demonstrate experimentally that Janssen's results can be generalized to a grain packing moving with respect to solid walls at velocities up to several  $\text{cm s}^{-1}$ .

A packing of 2 mm diameter glass beads (density  $\rho = 2.53 \cdot 10^3 \text{ kg m}^{-3}$ ) is contained inside a vertical glass tube of length 400 mm and internal diameter  $D = 30 \text{ mm}$ . This tube can be moved up and down at a chosen velocity  $v$  ranging from  $10 \mu\text{m s}^{-1}$  to  $35 \text{ mm s}^{-1}$ . A cylindrical piston of height 80 mm and diameter 29 mm is inserted in the bottom part of the tube: it is carefully aligned with it and does not touch the walls during the motion. The bottom end of the piston is screwed onto a strain gauge sensor connected to a lock-in detector allowing one to determine the force of the beads on the upper horizontal surface of the piston (Fig. 1). This value is divided by the gravitational acceleration  $g$  to obtain an apparent mass  $M_{\text{app}}$  determined with an uncertainty of  $\pm 0.1 \text{ g}$ . This apparent mass can be compared to the actual mass  $M$  of the grains measured by electronic scales prior to

the experiment, with a precision of  $\pm 0.01 \text{ g}$ . In addition, qualitative observations are realized using a video camera fitted with a macro lens and connected to a video tape recorder. The experiments were performed at a relative humidity  $H = (50 \pm 5)\%$ . For each experimental run, the

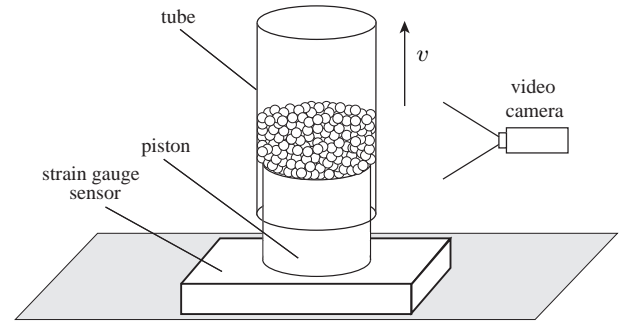


FIG. 1: Sketch of the experiment.

tube is first brought to its low position and filled with a given mass of beads  $M$ , using a funnel placed at the top of the tube. The relative motion between the grains and the walls is then induced by moving the tube upwards over a distance  $\Delta z \simeq 70 \text{ mm}$ . In the initial and final phases of the motion, the acceleration is equal to  $0.04 \text{ m s}^{-2}$  (or to  $0.055 \text{ m s}^{-2}$  for  $v = 35 \text{ mm s}^{-1}$ ) and the velocity  $v$  is constant in between. At the fastest velocity, the acceleration and deceleration distances are of order 11 mm and decrease to less than  $10^{-2} \text{ mm}$  for  $v < 1 \text{ mm s}^{-1}$ . One expects that, in the constant velocity phase, the relative motion of the grains with respect to the walls (and the force distribution) will be identical to those for a steady downwards grain flow in a tube at rest. The two control parameters of the experiment are the mass  $M$  of the grains poured into the tube and the tube velocity  $v$ . Compared to the flow of grains inside a static tube, the relative motion of grains and of the walls is the same but both the accelerations in the initial and final phases and the flow of air differ. Air flow should however have a weak influence since pressure gradients in these stationary compact grain flows are generally small.

Figure 2 displays variations of the apparent mass  $M_{\text{app}}$  as a function of time for seven identical exper-

iments. The mass of the grains initially poured into the tube is  $M = 300$  g and corresponds to a height  $h = (262 \pm 1)$  mm of the grain packing. Values of the ap-

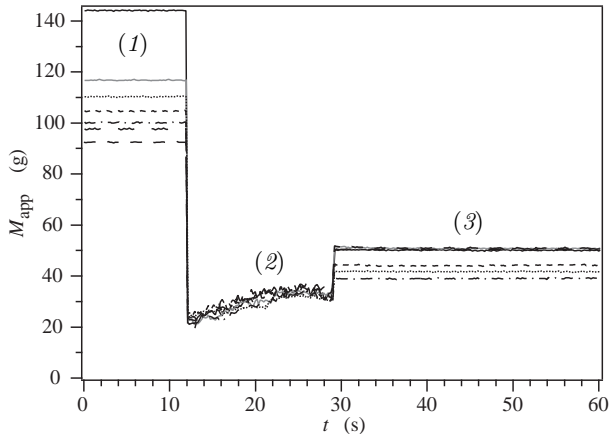


FIG. 2: Variation of the apparent mass  $M_{\text{app}}$  of a grain packing of total mass  $M = 300$  g as a function of time: (1) right after filling the tube, (2) tube moving upwards ( $v = 4$  mm s $^{-1}$ ), (3) tube stopped. Various line patterns correspond to different experiments realized with same control parameters.

parent mass  $M_{\text{app}}$  of the static packing right after filling the tube (region (1) in Fig. 2) are dispersed: the deviation is of the order of  $\pm 25\%$  of the mean value for large heights [16, 17]: they are explained by the heterogeneous stress network created when pouring the grains into the tube. Arches of grains appear at random inside the packing and screen the weight of other grains located above. These effects vary strongly from one sample to another, resulting in large variations of  $M_{\text{app}}$ .

At the onset of the tube motion, the apparent mass decreases abruptly and a random motion of the beads is observed. Then,  $M_{\text{app}}$  increases slightly during the constant velocity phase (region (2) in Fig. 2) and reaches a limiting value referred to in the following as  $M_{\text{app}}^{\text{dyn}}$ . A striking feature is the fact that  $M_{\text{app}}^{\text{dyn}}$  does not vary by more than  $\pm 5\%$  of its mean value from one sample to another. Figure 2 also shows that the time dependence is the same for all experiments within experimental uncertainty. When the tube stops (region (3) in Fig. 2), the apparent mass increases sharply to a constant value  $M_{\text{app}}^{\text{stat}}$  that is still much lower than in phase (1). The relative dispersion of these last static values is again quite large ( $\pm 15\%$ ). Moreover, one observes that the values of the apparent mass in region (1) and region (3) are not correlated. These experiments were repeated for different total masses  $M$  of grains and different tube velocities  $v$ . The respective experimental mean final values of  $M_{\text{app}}$  after it has become constant in region (2) and after the tube has stopped (region 3) are plotted in Fig. 3.

The apparent mass  $M_{\text{app}}^{\text{dyn}}$  at the end of the moving phase (dark symbols), is almost independent of the ve-

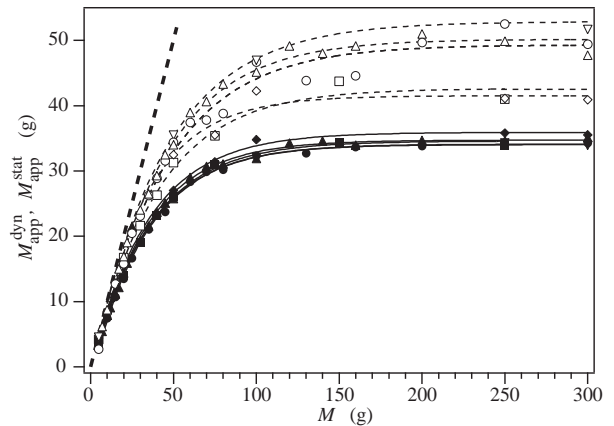


FIG. 3: Apparent mass as a function of total mass  $M$  of grain packing for different tube velocities: ( $\diamond, \blacklozenge$ )  $v = 0.02$  mm s $^{-1}$ , ( $\square, \blacksquare$ )  $v = 0.2$  mm s $^{-1}$ , ( $\circ, \bullet$ )  $v = 2$  mm s $^{-1}$ , ( $\triangle, \blacktriangle$ )  $v = 20$  mm s $^{-1}$ , ( $\nabla, \blacktriangledown$ )  $v = 34$  mm s $^{-1}$ . Each line corresponds to an exponential fit of the data points at each velocity. Dark symbols: limit value  $M_{\text{app}}^{\text{dyn}}$  at the end of region (2) (moving tube) ( $\Delta M_{\text{app}}^{\text{dyn}} = \pm 1$  g). Open symbols: apparent mass  $M_{\text{app}}^{\text{stat}}$  in region (3) (stopped tube) ( $\Delta M_{\text{app}}^{\text{stat}} = \pm 8$  g). Dashed thick line:  $M_{\text{app}} = M$ .

locity for all total masses  $M$  of grains in the tube. At low values of  $M$ , one has  $M_{\text{app}}^{\text{dyn}} \simeq M$  (there is no screening effect). Then the curve levels off and  $M_{\text{app}}^{\text{dyn}}$  reaches a limit value  $M_{\infty} = (34.5 \pm 1)$  g, independent of  $v$ .

After the tube motion has stopped (region 3), the apparent mass increases by 20 to 60% (open symbols) as already noted on Fig. 2. This increase is larger at higher velocities, but the final value is always lower than in region (1). The global shape of the variation of  $M_{\text{app}}^{\text{stat}}$  with  $M$  is qualitatively similar to that obtained for  $M_{\text{app}}^{\text{dyn}}$ , although the dispersion of the data points is much higher.

Video recordings of the grain packing during the experiments allowed one to estimate variations of the mean global particle fraction  $c$  in the sample: no systematic motion of the upper interface was detected and  $c$  remained constant with  $c = (64 \pm 0.5)\%$  in all experiments. These results indicate that the motion of the walls reorganizes the internal structure of the column: it allows to reach always a same statistical dynamical equilibrium in spite of the variability of the force distribution in the initial grain packing. This reorganization results from very minute motions since no variation of  $c$  is detected. Bringing the walls to rest perturbs the stress distribution and leaves the system “frozen” in a state which may vary significantly from one sample to another. As could be expected, the perturbation is larger at high velocities.

The curves of Fig. 3 follow *qualitatively* the predictions of Janssen’s model for static packing. We investigated therefore whether the *quantitative* predictions were also verified. The model assumes that the weight of the beads is balanced by variations of the stress  $\sigma_{zz}$  in the

vertical direction  $z$  and by wall friction with:

$$\frac{d\sigma_{zz}}{dz} + \frac{1}{\lambda}\sigma_{zz} = \rho cg, \quad (1)$$

where  $c$  is the local particle fraction of beads and  $\lambda = D/4\mu K$  a characteristic length. The coefficient  $K$  characterizes the deflection of vertical stresses into horizontal radial ones in the packing and  $\mu$  is the Coulomb friction coefficient. Integrating between the bottom ( $z = z_0$ ) and the surface ( $z = 0$ ) of the packing where  $\sigma_{zz}(0) = 0$ , gives the stress  $\sigma_{zz}(z_0)$  on the piston:

$$\sigma_{zz}(z_0) = \rho cg\lambda(1 - e^{-z_0/\lambda}). \quad (2)$$

Since  $M_{\text{app}} = \sigma_{zz}(z_0)\pi D^2/4g$  and  $M = \rho cz_0\pi D^2/4$ , it follows that:

$$M_{\text{app}} = M_{\infty}(1 - e^{-M/M_{\infty}}), \quad (3)$$

where  $M_{\infty}$  is the predicted asymptotic value of the apparent mass  $M_{\text{app}}$  when  $M$  is increased:

$$M_{\infty} = \rho c\lambda\pi D^2/4. \quad (4)$$

The solid and dashed lines in Fig. 3 represent respectively the best fit with Eq. (3) of experimental data points obtained during and after the motion of the tube. The fits are excellent in the first case and fair in the second one due to the larger dispersion of the data points. These fits allow one to determine the asymptotic apparent mass  $M_{\infty}$  and the characteristic length  $\lambda$  of Janssen's model. Variations with the tube velocity  $v$  of  $\lambda$  values corresponding to both sets of data are displayed in Fig. 4. In

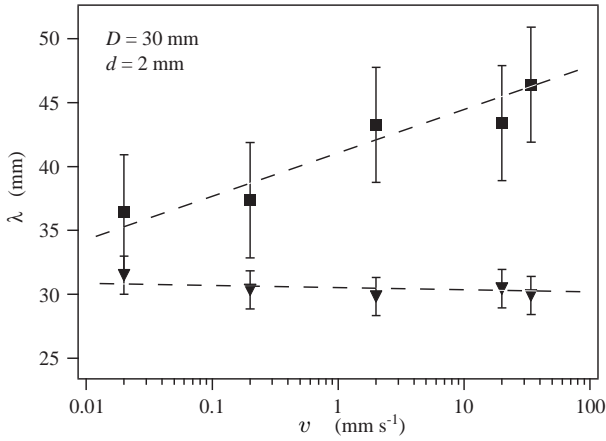


FIG. 4: Janssen's length variations with the tube velocity: (▼) during the flow, (■) after the tube stops.

the moving phase,  $\lambda$  remains at the nearly constant value  $\lambda = (30 \pm 2)$  mm. This value is close to the tube diameter ( $D = 30$  mm) and two or three times lower than estimates in region (1) from Eq. (4). After the tube has been stopped (region 3),  $\lambda$  is nearly the same as in region (2)

at the lowest velocity but increases by 30% at the highest one. This confirms that perturbations of the stress distribution induced by stopping the tube are larger at higher velocities. A part of the arches and of the contacts between grains probably disappear, which reduces the value of the coefficient  $K$  (and therefore increases  $\lambda$ ).

Another important issue is the dynamics of the grain rearrangement while the tube is moving. This can be inferred from variations of the apparent weight during the motion of the tube. Figure 5 displays superimposed variations of  $M_{\text{app}}/M_{\text{app}}^{\text{dyn}}$  as a function of the normalized displacement  $z/D$  for several velocities ranging from  $40 \mu\text{m s}^{-1}$  to  $34 \text{ mm s}^{-1}$ . The total mass of grains is equal to  $M = 300$  g for which  $M_{\text{app}}^{\text{dyn}} = M_{\infty} = 34.5$  g. A common

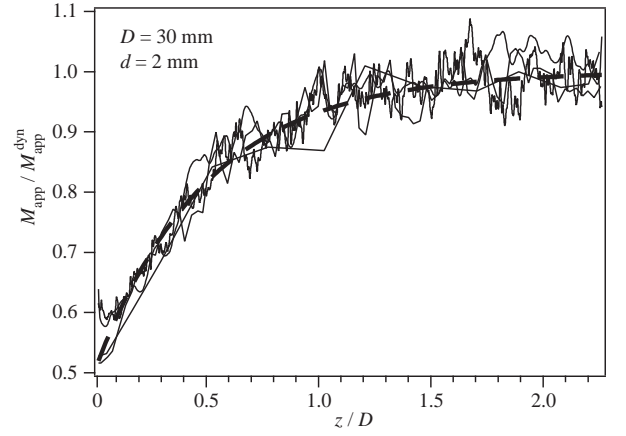


FIG. 5: Variation of the normalized apparent mass  $M_{\text{app}}/M_{\text{app}}^{\text{dyn}}$  with the normalized displacement  $z/D$ , at velocities  $40 \mu\text{m s}^{-1} \leq v \leq 34 \text{ mm s}^{-1}$ .

increasing trend is followed and is well adjusted by an exponential variation (dashed line):

$$\frac{M_{\text{app}}}{M_{\text{app}}^{\text{dyn}}} = 1 - A \exp\left(-\frac{\alpha z}{D}\right), \quad (5)$$

with  $A = 0.48$  and  $\alpha = 2 \pm 0.2$ . The characteristic relaxation length towards the limit value  $M_{\text{app}}^{\text{dyn}}$  in Fig. 5 is equal to  $D/2$ . The sharp drop of  $M_{\text{app}}$  right after the onset of the motion implies that grains are initially dragged upwards (a small transient motion is observed on video recordings); then, the packing rearranges and more contact paths build-up towards the sensor at the bottom.

The influence of the tube diameter  $D$  has been investigated by performing the experiments on a tube of larger diameter  $D = 40$  mm (beads of diameter  $d = 3$  mm are used to keep  $D/d$  roughly constant). As for  $D = 30$  mm, the variation of  $M_{\text{app}}/M_{\text{app}}^{\text{dyn}}$  with  $z/D$  is almost independent on the tube velocity (Fig. 6).  $M_{\text{app}}$  increases also exponentially with the displacement  $z$ , following Eq. (5) with the same value of the parameter  $\alpha$ , as for  $D = 30$  mm ( $A = 0.39$  and  $\alpha = 2 \pm 0.3$ ). This indicates that the rearrangement depends mostly on the normalized displacement  $z/D$ . The variation of  $M_{\text{app}}$  with  $M$  also verifies

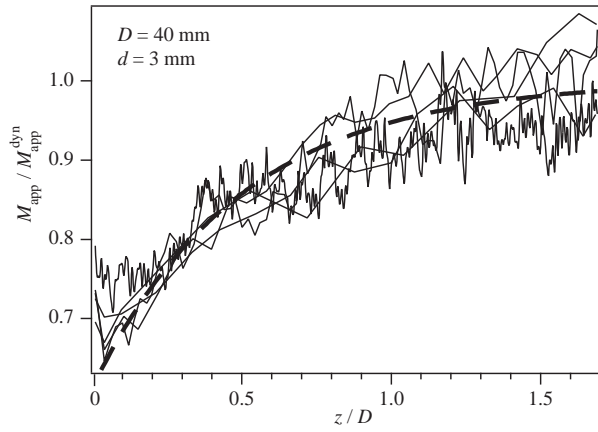


FIG. 6: Variation of the normalized apparent mass  $M_{\text{app}}^{\text{dyn}}/M_{\text{app}}$  with the normalized displacement  $z/D$ , at velocities  $0.4 \text{ mm s}^{-1} \leq v \leq 34 \text{ mm s}^{-1}$  ( $M = 300 \text{ g}$ ,  $M_{\text{app}}^{\text{dyn}} = M_{\infty} = 98 \text{ g}$ ).

Eq. (3): the corresponding shielding length is independent of velocity with  $\lambda = (48 \pm 4) \text{ mm}$ . As expected,  $\lambda$  increases with  $D$ ; experiments for a broader range of values of  $d$  and  $D$  will be necessary to establish the dependence of  $\lambda$  on these parameters and on the ratio  $D/d$ .

Preliminary experiments were performed at a lower relative humidity ( $H \lesssim 40\%$ ). On the one hand, the variations of  $M_{\text{app}}$  with the total mass  $M$  remain in agreement with Janssen's model and both the mean  $M_{\text{app}}$  values and their relative dispersion are still much smaller than for the initial static packing. These mean values are also of the same order as before. On the other hand,  $M_{\text{app}}$  remains constant in region (2) instead of increasing towards a limit value as previously. At the same time, grains remain at rest on the outside of the packing while the tube moves. These results imply that friction forces on the grains are smaller for  $H \simeq 40\%$ ; they also indicate that even invisible rearrangements of the packing during the wall motion may induce large changes of the force distribution. Note that all experimental data presented here were obtained after an equilibrium of humidity between air and the grains had been reached.

These results indicate that the grain packing reaches a dynamical equilibrium independent of the initial state and of the relative velocity with respect to the walls: frequent transitions between different force distributions in the packing are induced by the tube motion leading to a well defined average value. These distributions are sensitive to small motions of the grains: these do not induce measurable variations of the mean particle fraction and are not even observable visually in some cases. The dynamical equilibrium is reached exponentially with a characteristic length proportional to the tube diameter: this may be due to the fact that the reorganization of the grains starts at the walls and propagates thereafter towards the center of the tube. Stopping the flow

increases  $M_{\text{app}}$ , particularly at large velocities, but it remains smaller than the initial value after filling. The variability of  $M_{\text{app}}$  from one experiment to another is much greater than during the tube motion since the system is “frozen” in one state and the averaging effect of the variations of the force distributions has disappeared.

To conclude, the present experiments demonstrate that Janssen's model remains valid up to velocities of several centimeters per second for granular packing inside a vertical tube in motion with respect to the grains. The apparent mass  $M_{\text{app}}$  measured at the bottom of the packing during the tube motion is much smaller than for the initial static packing. The limiting value of the apparent mass at the end of the moving phase ( $M_{\text{app}}^{\text{dyn}}$ ) is also independent of the tube velocity  $v$  and much less variable from a sample to another than for static packings (for a given total mass of the grains). Globally, the result of this study suggests that force distributions in dense granular flows may be described by straightforward models over a much broader range of velocities than usually expected.

We thank B. Perrin for many helpful discussions, H. Auradou and L. Biver for their contribution to the experiments and G. Chauvin, Ch. Saurine and R. Pidoux for the realization of the experimental setup. We thank Ph. Gondret for a thoughtful reading of the manuscript.

- 
- [1] S. Laouar and Y. Molodtsov, *Powder Technol.* **95**, 165 (1998).
  - [2] J. Duran, *Sands, powders and grains. An introduction to the physics of granular materials.* (Springer-Verlag, 2000).
  - [3] P. G. de Gennes, *Rev. Mod. Phys.* **71**, 374 (1999).
  - [4] H. A. Janssen, *Z. Ver. Dtsch. Ing.* **39**, 1045 (1895).
  - [5] J. P. Bouchaud, M. E. Cates, and P. Claudin, *J. Phys. I France* **5**, 639 (1995).
  - [6] C. C. Mounfield and S. F. Edwards, *Physica A* **226**, 12 (1996).
  - [7] D. M. Mueth, H. M. Jaeger, and S. R. Nagel, *Phys. Rev. E* **57**, 3164 (1998).
  - [8] E. B. Pitman, *Phys. Rev. E* **57**, 3170 (1998).
  - [9] L. Vanel, P. Claudin, J. P. Bouchaud, M. E. Cates, E. Clément, and J. P. Wittmer, *Phys. Rev. Lett.* **84**, 1439 (2000).
  - [10] G. Ovarlez, E. Kolb, and E. Clément, *Phys. Rev. E* **64** (2001).
  - [11] O. Pouliquen and R. Gutfraind, *Phys. Rev. E* **53**, 552 (1996).
  - [12] S. F. Edwards and C. C. Mounfield, *Physica A* **226**, 25 (1996).
  - [13] C. Eloy and E. Clément, *J. Phys. I France* **7**, 1541 (1997).
  - [14] J. Rajchenbach, *Phys. Rev. E* **63** (2001).
  - [15] L. Vanel and E. Clément, *Eur. Phys. J. B* **11**, 525 (1999).
  - [16] J. Duran, E. Kolb, and L. Vanel, *Phys. Rev. E* **58**, 805 (1998).
  - [17] L. Vanel, D. Howell, D. Clark, R. P. Behringer, and E. Clément, *Phys. Rev. E* **60**, R5040 (1999).